Solid Freeform Fabrication 2017: Proceedings of the 28th Annual International Solid Freeform Fabrication Symposium – An Additive Manufacturing Conference
Reviewed Paper

Effect of Constrained Surface Texturing on Separation Force in Projection Stereolithography

Haiyang He[1], Yayue Pan *[1], Jie Xu[1], Xiaoming Yu[2]

1 Department of Mechanical and Industrial Engineering, University of Illinois at Chicago, Chicago, IL, 60607, USA

2 College of Optics &Photonics, University of Central Florida, Orlando, FL, 32816, USA

Abstract

In projection stereolithography (SL) processes, the separation of a newly cured layer from the constrained surface is a historical technical barrier and still greatly limits its printable size, process reliability and print speed. This paper presents an approach to reduce the separation force in projection stereolithography (SL) processes by texturing the constrained surface with radial microgroove patterns. Separation forces with conventional smooth constrained surface and textured surface are both modeled. The analytical model suggests that a proper design of micro patterns of the constrained surface is capable of reducing separation forces greatly. Furthermore, a projection SL testbed with online separation force monitoring unit is developed for experimental study. Experimental results verified the effectiveness of micro surface textures in reducing separation forces. Test cases also show that with the help of the proposed textured constrained surface, parts with wide solid cross sections that could not be printed using conventional methods were manufactured successfully. The influence of the textured constrained surface on the printed parts' surface roughness is studied, a grey scale projection approach is proposed to eliminate the influence and improve the surface quality of printed parts. Hence, the presented methods can help to improve the manufacturing capability of Projection SL processes.

Keywords: Additive Manufacturing, Projection Stereolithography, Surface Texture, Constrained Surface.

Introduction

Projection Stereolithography (SL) is one of the most important Additive Manufacturing technologies currently available and also the first commercialized AM technology. In Projection SL process, liquid photosensitive polymer is cured usually through the use of a DLP projector, which supplies the amount of energy via projecting digital mask images to induce a curing reaction, forming a highly cross-linked polymer. Compared to other polymer additive manufacturing techniques like extrusion or jetting processes, Projection SL produces parts with the highest accuracy and the best surface finish.

There are two ways to cure liquid polymer in Projection SL, free surface method and constrained surface method, as illustrated in Fig.1. Compared to free surface process, the constrained surface process has several advantages including less material waste, higher resolution and faster speed, and is being used increasingly recently. Despite the advantages, the separation of a newly cured layer from the constrained surface is a historical technical barrier and still greatly limits the printable size, process reliability and print speed [1].

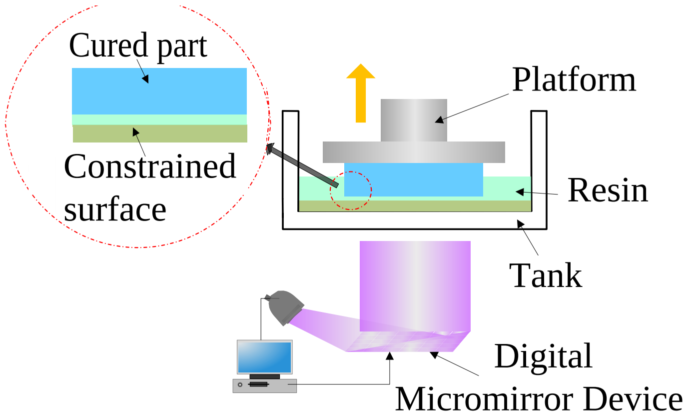

Figure 1. A schematic diagram of constrained surface based Projection SL

As illustrated in Fig. 1, in constrained surface Projection SL process, the separation force occurs in the process of lifting newly cured layer up and refilling liquid resin into the gap created during lifting process. Hence, the separation force exerted on newly cured layer is actually the suction force caused by pressure difference in liquid filling[[2]].

Extensive research has been conducted to reduce separation forces. Approaches like peeling, two-way movement, and coating have been developed. However, these approaches may prolong total the build time, require much larger liquid tank, and frequent replacements of coatings [3, 4]. The peeling approach introduces other problems like corrugated constrained surfaces and large peeling force [5, 6]. These drawbacks are more significant when the print area is large. Hence separation problem still remains to be the primary challenge and limits the manufacturing capability of Projection SL. For example, it is worth noting that building envelopes of current Projection SL machines are all in inch level, and no greater than 8 L x 5 W x 10 H. To produce a part in feet level is almost impossible. Therefore, it is of highly significance to reduce the separation force and enhance the capability of Projection SL.

Against this background, this paper aims to develop novel approaches to reducing separation forces, without sacrificing other properties like speed, volume and reliability. A constrained surface texturing approach for separation force reduction is developed in this study.

1. Effects of Constrained Surface Texture on Separation Force

In constrained surface SL, conditions of the interfaces, the newly cured layer surface and constrained surface, play important roles in determining separation forces. In addition, surface texturing has been widely used for altering pressure gradient or liquid flow dynamics in various applications [7, 8, 9, 10, 11], but not yet in constrained surface design for stereolithography. Hence, in this study, we investigate how to modify the constrained surface to reduce separation forces in SL process.

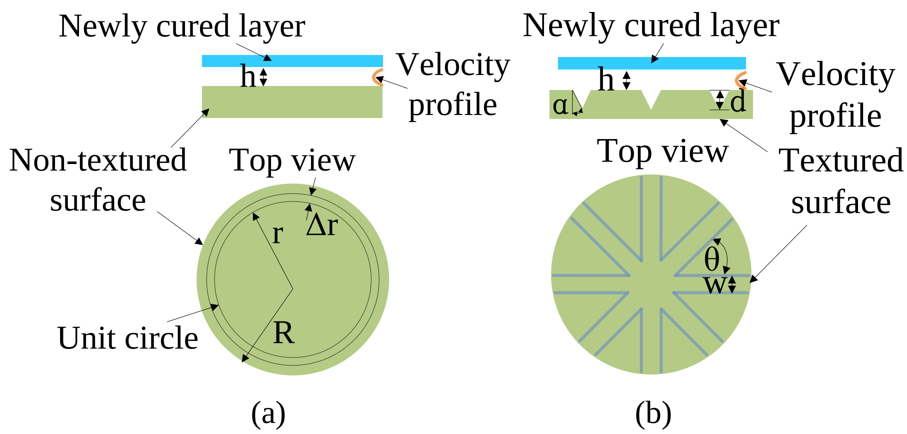

Figure 2. Schematic of separation areas with a solid circular layer and (a) non-textured constrained surface (b) textured constrained surface

Fig. 2 (a) shows a schematic diagram of the separation area in conventional Projection SL systems based on smooth constrained surface. R is the radius of the part, and h is the height of the gap between the newly cured layer and the coating. Fig. 2(b) is a schematic of separation area with proposed constrained surface, which is patterned with a radial microgroove pattern. The microgroove pattern has four design parameters: groove width w, groove depth d, the angle of each groove is α and groove radial distance θ.

To investigate effects of surface texture on separation forces and learn how to design parameters, the liquid filling process and separation force are modelled for both conventional smooth surface and textured surface.

<u>**Separation force with smooth constrained surface**</u>:

By applying Navier–Stokes equations, we can get:

$$\boldsymbol{\mu} \frac{\partial^2 \boldsymbol{u}}{\partial \boldsymbol{z}^2} = \frac{\boldsymbol{dP}}{\boldsymbol{dr}} \tag{1}$$

where μ is the viscosity of the liquid. Based on Mass Conservation Equation, the relationship between the Z stage moving speed $\boldsymbol{V}$ and liquid flow rate $\boldsymbol{Q}$ can be found:

$$\boldsymbol{Q} = \boldsymbol{V} \cdot \boldsymbol{\pi} \cdot \boldsymbol{r}^2 = 2 \cdot \boldsymbol{\pi} \cdot \boldsymbol{r} \int_0^h \boldsymbol{u} \boldsymbol{dz} \tag{2}$$

By substituting (1) into(2), the pressure gradient Δp and resulted pressure $\boldsymbol{P}$ could be derived as:

$$\Delta \boldsymbol{p} = \boldsymbol{V} \mu \boldsymbol{r} \cdot \frac{6}{\boldsymbol{h}^3} \tag{3}$$

$$\boldsymbol{P} = -\frac{3\mu \boldsymbol{V}}{\boldsymbol{h}^3} \cdot \boldsymbol{r}^2 + \frac{3\mu \boldsymbol{V}}{\boldsymbol{h}^3} \cdot \boldsymbol{R}^2 \tag{4}$$

Thus, the separation force $\boldsymbol{F}$ exerted on part can be calculated by integrating the pressure across the area:

$$F = \int_0^R 2\pi r P\, dr = \frac{3\pi \cdot \mu V}{2 \cdot h^3} \cdot R^4 \quad (5)$$

Separation force with textured constrained surface:

According to [12], the hydraulic resistance R_{hyd} for straight channels with arbitrary cross-sectional shape could be approximated by:

$$R_{hyd} \approx 2 \cdot \mu \cdot L \cdot \frac{Pe^2}{A^3} \quad (6)$$

where L is the channel length, μ the dynamic viscosity of the liquid, A the cross-sectional area and Pe the perimeter. Also, by definition, the hydraulic resistance is:

$$R_{hyd}(\Delta p) \equiv \frac{\Delta p}{Q(\Delta p)} \quad (7)$$

where Δp is a certain pressure drop and Q is the flow rate.

From (6) and (7), we can obtain:

$$\Delta p = \frac{dp}{dr} = Q \cdot 2\mu \cdot \frac{Pe^2}{A^3} \quad (8)$$

For situation with micro textures,

$$Pe = 2 \cdot 2\pi \cdot r + 2 \cdot n \cdot \left(\frac{d}{\cos(\alpha/2)} - \frac{w}{2}\right) \quad (9)$$

$$A = 2\pi \cdot r \cdot h + 0.5n \cdot w \cdot d \quad (10)$$

$$Q = V \cdot \pi \cdot r^2 \quad (11)$$

where V is the separation speed, n the number of grooves. w and d are the width and depth of the grooves. h denotes the height of the gap.

By substituting (9), (10) and (11) into(8), we can obtain

$$\frac{dp}{dr} = V \cdot \pi r^2 \cdot 2\mu \cdot \frac{\left(2 \cdot 2\pi \cdot r + 2 \cdot n \cdot \left(\frac{d}{\cos(\alpha/2)} - \frac{w}{2}\right)\right)^2}{(2\pi \cdot r \cdot h + 0.5n \cdot w \cdot d)^3} \quad (12)$$

By taking integral of the pressure p on each unit circle, the separation force could be calculated. To investigate the effects of microgrooves on separation force reduction, pressure gradient is calculated for textured surface using Equation (12), and then compared with pressure gradient for smooth surface in Equation (3). It was found that textured surface will reduce pressure drop by ~60% compared with conventional smooth surface when other conditions are restricted the same and hence smaller separation force than those of smooth PDMS.

To achieve smallest separation force, the pressure drop should be lowest. Thus, by taking the partial derivative of the pressure drop with respect to w in equation (12), we can get:

$$\frac{\partial \Delta p}{\partial w} = 2\mu V \pi r^2 \frac{\left[-2n\left(4\pi r + \frac{2nd}{\cos(\alpha/2)} - nw\right)(2\pi r h + 0.5ndw) - 1.5nd\left(4\pi r + \frac{2nd}{\cos(\alpha/2)} - nw\right)^2\right]}{(2\pi r h + nwd)^4} \quad (13)$$

Since w, d, n and h are all larger than zero and $4\pi r >> nw$, above equation cannot be zero.

Similarly, take the partial derivative of the pressure drop with respect to d in equation (12),

$$\frac{\partial \Delta p}{\partial d} = 2\mu V \pi r^2 \frac{\frac{4n}{cos(\alpha/2)}\left(4\pi r + \frac{2nd}{cos(\alpha/2)} - nw\right)(2\pi rh + 0.5nwd) - 1.5nw\left(4\pi r + \frac{2nd}{cos(\alpha/2)} - nw\right)^2}{(2\pi rh + nwd)^4} \quad (14)$$

Set $\frac{\partial \Delta p}{\partial d} = 0$

$$d = \frac{16\pi rh + 3nw^2 cos(\alpha/2) - 12\pi rw cos(\alpha/2)}{2nw} \quad (15)$$

Therefore, the micro texture height and width, d and w should be designed based on the relationship described in equation (15) for achieving the smallest separation force.

Based on the study in [13], the oxygen inhibition layer thickness above a PDMS film is ~2 µm. Thus, when h is fixed at 2 µm, the relationship between the width and depth of the micro textures is shown in Figure 3. The relationship above can be used as a guide when designing the parameters of the textures on PDMS.

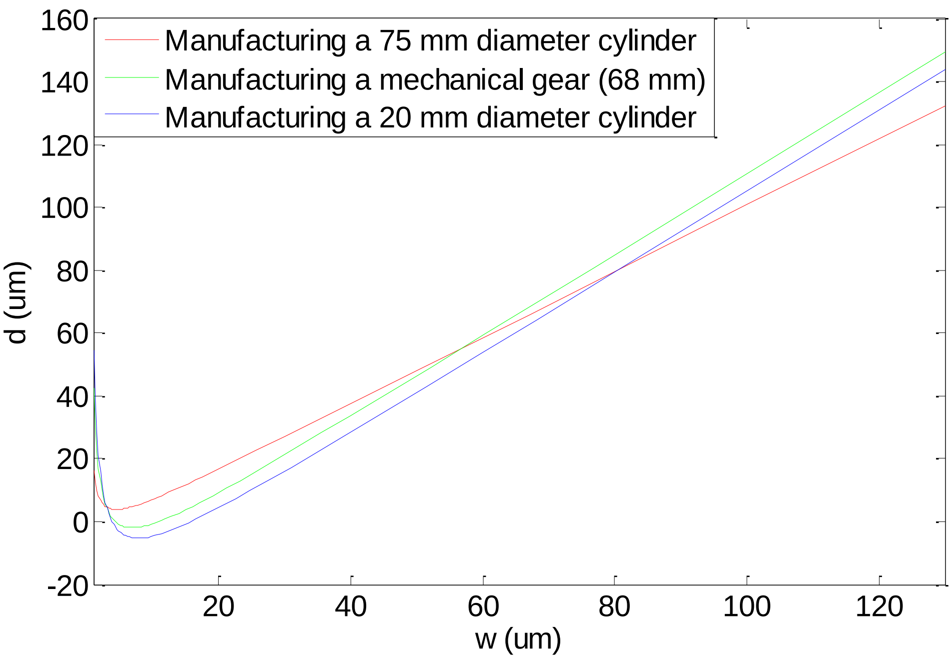

Figure 3. The relationship between width and depth of micro textures for achieving the smallest separation force

2. Textured Constrained Surface based Projection SL Experimental Setup

As shown in Fig. 4, a constrained surface based Projection SL testbed is built. The setup consists of an imaging unit, a resin vat which is an optic clear petri dish, a linear actuator that elevates the build platform, a control board, and a load cell that measures the separation force. The load cell is mounted directly on the platform, so real-time force can be measured and recorded. An off-the-shelf projector is used as the imagining unit. The optical lenses of the projector were modified to reduce the projection distance. Various projection settings, including focus, key stone rectification, brightness, and contrast were adjusted to achieve a sharp projection image on the projection plane. A process control testbed has been developed using C++ language. It integrates the geometry slicing, image projection, and motion controlling. In addition, an online force monitoring testbed has been developed in Matlab. It reads and processes data from the load cell, and saves the separation force in real time.

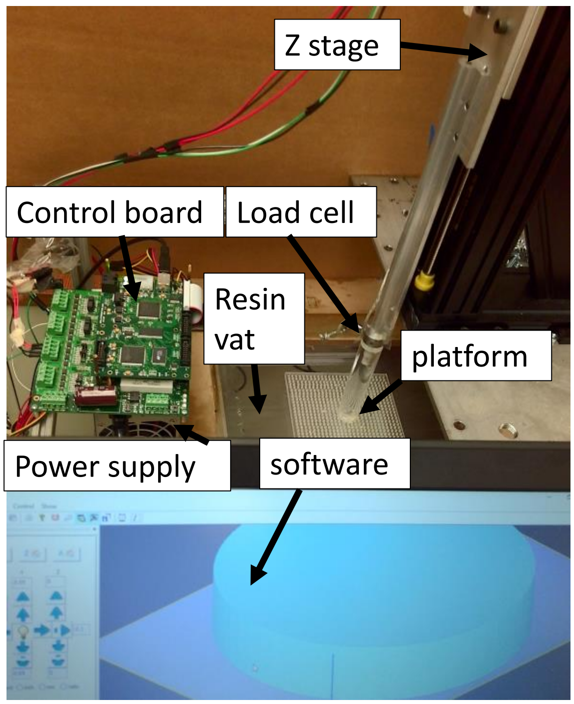

Figure 4. Hardware Setup

Conventional Projection SL systems are usually based on smooth Polydimethylsiloxane (PDMS) films or smooth TEFLON films. In this study, PDMS films are prepared and coated on bottom surfaces of the resin vat. To explore the potential of textured constrained surface in reducing separation forces, both conventional smooth PDMS films, and PDMS films with designed surface textures are tested.

3. Experimental Results and Discussions

3.1. PDMS Texturing and Force Measurements

Fig. 2 (b) is an illustration of the resin replenishment with a textured surface, where the constrained surface is patterned with radially symmetric microgrooves. Those microgrooves will help increase the flow pathway cross section, hence the resin flow rate. Micro patterns with different parameter settings, i.e. width and depth of the microgrooves, radius of the centre hole, have been prepared on 1mm thick PDMS substrates. Microscopic images of the top view of four samples are shown in Fig. 5, where the red scale bar is 0.2mm. Surface #1 was textured by micro-milling process, consisting of 8 radially symmetrical microgrooves, with 80µm width and 80µm depth. The other three surfaces were textured by using femtosecond (fs) laser micromachining technology, which utilized a 40-fs laser beam to fabricate the designed microgrooves with high precision. Details of the laser micromachining process can be found in [14]. The geometries of the microgrooves in these three samples are: #2-width 43 µm, depth 46 µm, angle 15º; #3-width 60 µm, depth 107 µm, angle 15º; #4-width 66 µm, depth 290 µm, angle 15º.

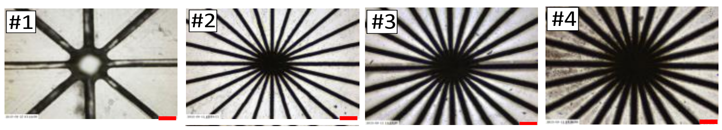

Figure 5. Microscopic images of four textured surfaces. Scale bar: 0.2mm.

Experiments were carried out to test the effectiveness of micro textures on separation force reduction. A solid cylinder with a radius of 10 mm has been built with the conventional Projection SL based on smooth constrained surface, and also with the proposed Projection SL based on the textured surface (#2-width 43 µm, depth 46 µm) as shown in Fig. 5. In all experiments, a velocity of Z elevator of 1.56 mm/s. an acceleration of Z elevator of 1.25 mm^2/s, and a layer thickness of 203.2 um are used. In addition, the same resin MakerJuice G+ with a viscosity of 90 cP is used in all tests.

Forces during printing in the developed SL testbed, with the two types of constrained surfaces, conventional smooth PDMS and textured PDMS surfaces, are measured. Fig. 6 plots forces in the process of printing 8 successive layers by using smooth surface and the four textured surface samples in Fig. 5. Compared to the conventional smooth PDMS surface, separation forces in the printing process are reduced by ~60% by using textured surfaces.

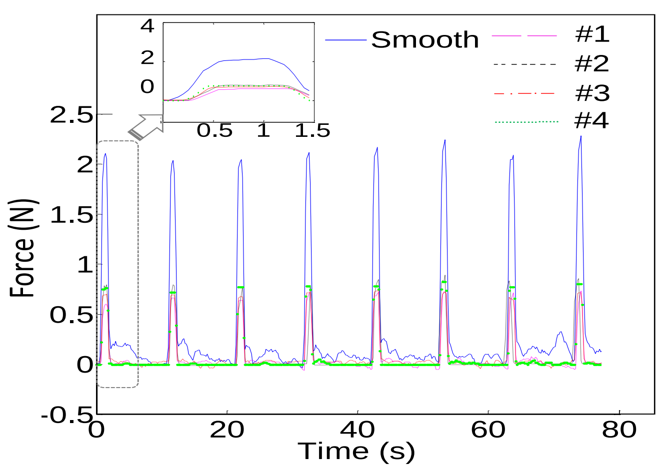

Figure 6. Separation forces during printing 8 layers by using non-textured PDMS film and the four textured PDMS films showed in Fig. 5.

Note that the PDMS surface also deforms in the separation forces. Hence the peak of separation force doesn't occur exactly in the initial moment of part elevation, and the actual separation velocity V is smaller than the Z stage velocity due to the deformation of PDMS surface. The experimental results verified that the separation force could be reduced greatly by modifying the constrained surface with radial microgroove textures.

3.2 Test Case 1: Fabrication of A Hand Model with Textured Constrained Surface Projection SL Technology

The effectiveness of textured surface on reducing separation forces were verified by comparing measured separation forces. To further validate the capability of Projection SL based on textured surfaces, multiple complicated structures have been fabricated using the developed testbed and textured surface sample #2. A hand model is printed using proposed approach. Its CAD model, fabricated picture, cross section contour and the corresponding microscopic image are shown in Fig. 7. The scale bar is 5 mm.

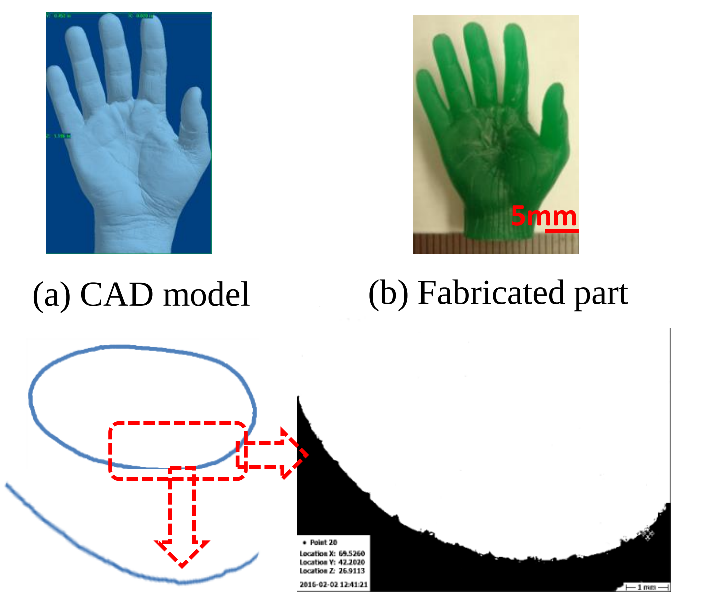

(a) CAD model (b) Fabricated part

(c) CAD contour of the wrist (d) Microscopic image of the fabricated wrist contour

Figure 7. A hand model printed with textured constrained surface.

3.3 Test Case 2: Fabrication of A ring model with Textured Constrained Surface Projection SL Technology

To validate the capability of the proposed approach for manufacturing parts with delicate features, a ring model is printed using textured sample #2. Its CAD model, fabricated picture, cross section contour and the corresponding microscopic image are shown in Fig. 8. The scale bar is 5 mm.

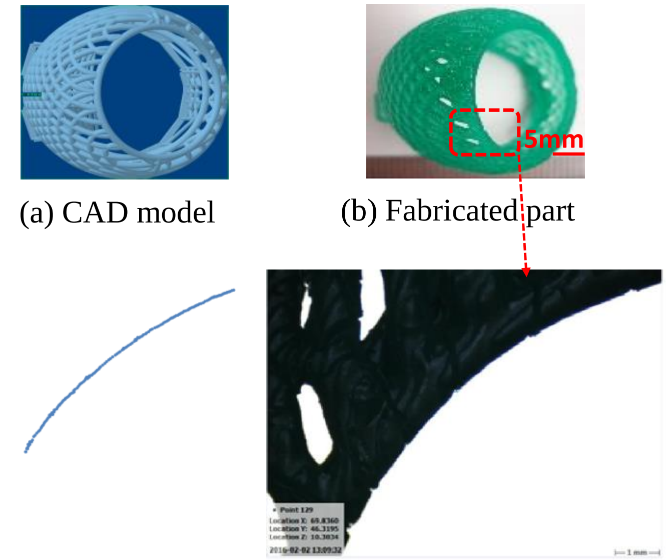

(a) CAD model (b) Fabricated part

(c) CAD contour segment of the ring (d) Microscopic image of fabricated part contour

Figure 8. A ring model printed with textured constrained surface

Although the conventional smooth PDMS surface can also print such parts of this size, the separation force will be much larger than that of textured PDMS, which will result in shorter life of the constrained surface. As the building size increases, there is a high risk that the increasing separation force will damage the parts or even fail the build process.

3.4 Test Case 3: Fabrication of a 75 mm diameter cylinder using Textured Constrained Surface

Printing geometry with a wide solid cross section has always been a challenge for constrained surface SL due to over-large separation force. To validate the effectiveness of textured surface PDMS constrained surface on fabricating objects with wide solid cross sections with small separation force, a 75mm diameter cylinder, was tested. The height of the cylinder is 25mm.

The material used for experiments is MakerJuice G+ (green). The layer thickness is set to be 50 um. The part was printed both in a commercial machine with smooth constrained surface and our prototype with textured constrained surface. With the commercial machine, the part failed during the printing process at around 1 mm in height. The failed part is shown in Fig. 9 (a). However, with the textured constrained surface, the printing job was successfully completed and the printed part is shown in Fig. 9 (b). The comparison between the failure part and our successful part is given in Fig. 9 (c).

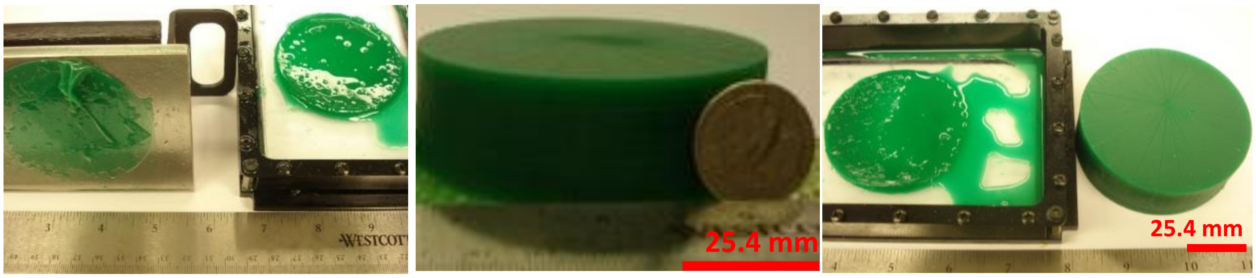

(a) (b) (c)

Figure 9. (a) Failure of printing a 75mm diameter cylinder using commercial machine. Part was pulled down from the platform due to large separation force and stick on the constrained surface (b) Success of Printing a 75mm cylinder using a textured constrained surface based testbed. (c) Comparison between the failed part stick on the constrained surface of the commercial machine and successfully printed part using the textured constrained surface

The separation force for building the part with textured surface was recorded and is plotted in Fig.10. The average separation force is ~18N for each layer. Besides, there is no significant increase of separation force over the manufacturing process, which is often seen in conventional constrained surface SL processes [15].

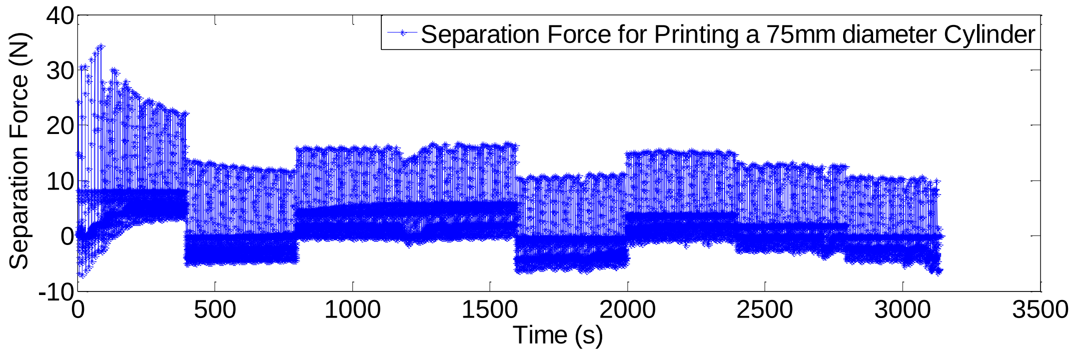

Figure 10. Separation force for printing a 75mm diameter cylinder using the textured constrained surface (~520 layers)

The cylinder's CAD model, fabricated picture, cross section contour and the corresponding microscopic image are shown in Fig. 11.

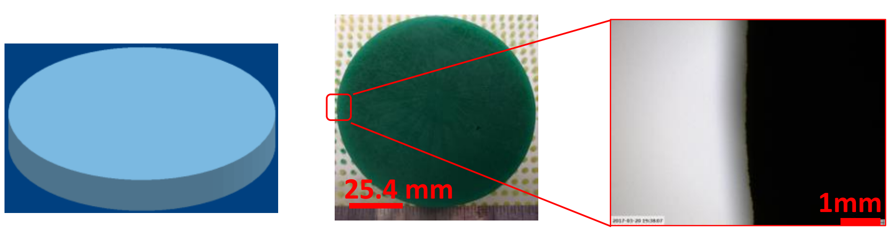

(a) CAD model (b) Fabricated part (c) Microscopic image

Figure 11. A 75 mm diameter cylinder printed with textured constrained surface

3.5 Test Case 4: Fabrication of Gear using Textured Constrained Surface

To further demonstrate the capability and versatility of textured constrained surface, a common mechanical gear (~68 mm diameter, 10mm in height) is printed. The material used is SL600M, produced by Envision TEC. The part was printed using both a commercial machine with conventional constrained surface and our setup with textured surface. After printing a few layers in the commercial machine, the part was pulled down from the platform by the large separation force and adhered to the constrained surface. Debris could be observed on the metal platform and the constrained surface, as shown in Fig. 12 (b).

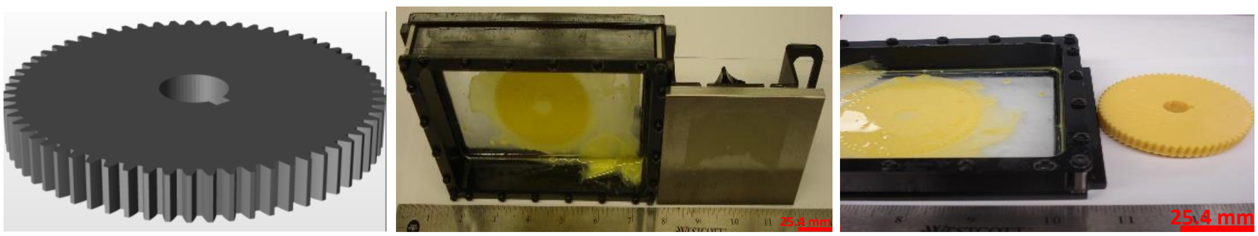

(a) (b) (c)

Figure 12. (a) A CAD model of a mechanical gear (b) Failure of printing a mechanical gear in a commercial machine which uses the conventional non-textured constrained surface (c) Comparison between the failed part printed in the commercial machine and the successfully printed part in our setup using textured constrained surface

However, with the textured surface, the gear can be successfully printed. The comparison between these two parts are given in Fig. 12 (c) (scale bar: 25.4mm). The separation force for manufacturing this gear with textured was recorded during the whole process, as plotted in Fig. 13.

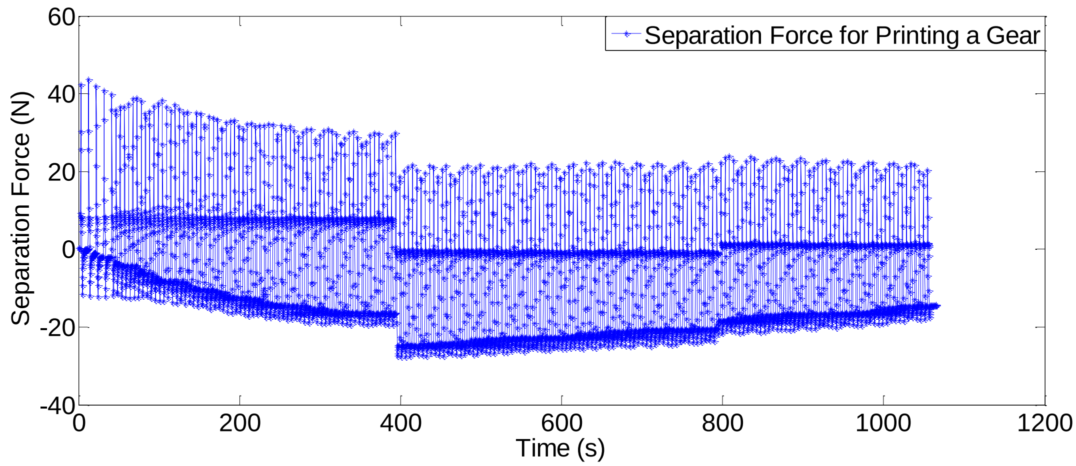

Figure 13. Separation force for printing the mechanical gear using the textured constrained surface (~200 layers)

The gear's CAD model, fabricated picture, cross section contour and the corresponding microscopic image are shown in Fig. 14.

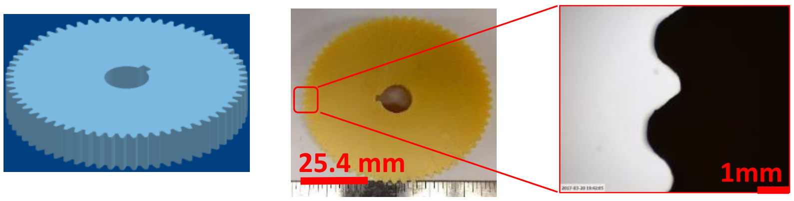

(a) CAD model (b) Fabricated part (c) Microscopic image

Figure 14. A gear printed with textured constrained surface

4. Discussion of Texture Imprinted on Part Surface

Although the textured constrained surface significantly reduced the separation force and enables successful prints of objects with wide solid cross sections, the textured constrained surface brings a surface finish problem. The textures were imprinted on the part surface and can be observed. To better understand the effects of textured constrained surface on surface finish of printed parts, this section characterizes the part surface finish and investigate approaches to eliminate the imprinted textures.

Eight samples were manufactured using the textured PDMS constrained surface, and two different resins, MakerJuice and SL500. Figure 15 (a) shows a sample and Fig. 15 (b) shows a microscopic image of the region that was printed by the micro-groove region of the PDMS film. As shown in Fig. 15 (b), the radial micro surface texture of the constrained surface was printed on the surface of the square part. Optical surface profilometer was used to characterize the imprinted textures. The profile of the line region in Fig. 15 (b) is plotted as the blue curve in Fig. 15 (e). It can be seen that the height of the texture is ~100 um, which is very close to the depth of the micro-groove on the PDMS surface.

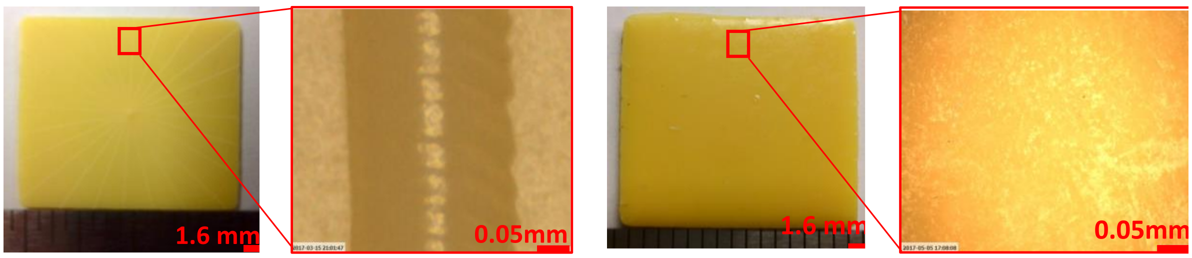

(a) (b) (c) (d)

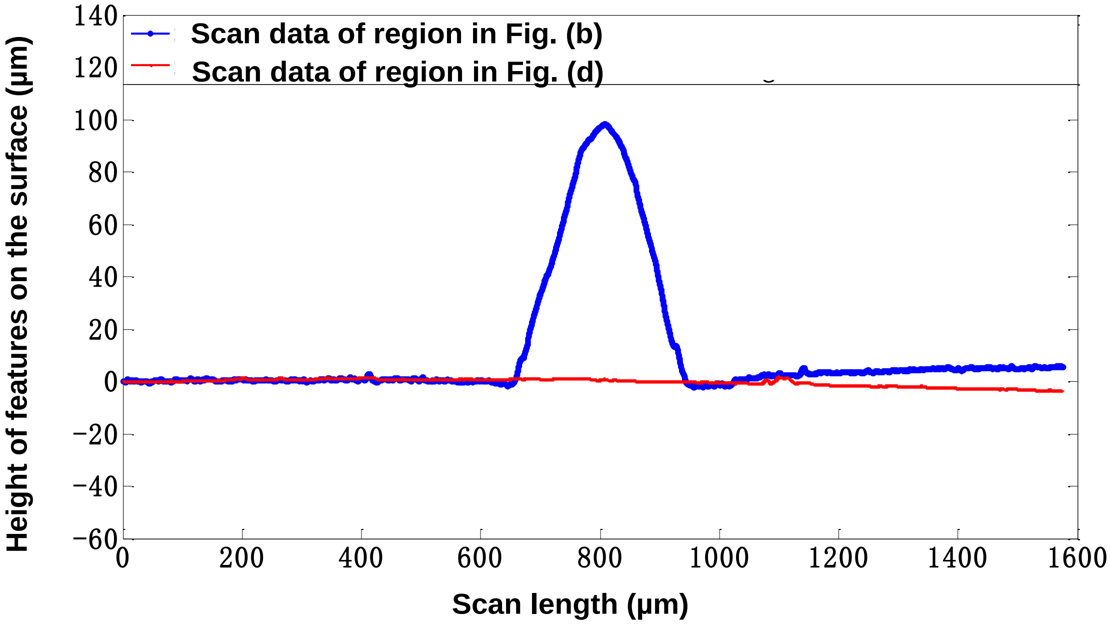

(e)

Figure 15. Samples printed with and without gray scale images: (a) a sample printed with the conventional mask image projection method; (b) microscopic image of the imprinted texture on the sample in (a); (c) a sample printed with the proposed gray scale image projection method; (b) microscopic image of the region where microtexture was imprinted; (e) Z profiles of the region of the part surface where was in contact with the micro-groove on the textured constrained surface.

To address this texture printing problem, a gray scale projection method was investigated. After curing a layer, a grey scale image (R: 110, G: 110, B: 110) of that layer is projected. Due to the oxygen inhibition adjacent to the constrained surface, only a thin film of resin will be cured on the layer in the non-textured regions. To test the feasibility of this method, the same square sample was printed using this gray scale image method. Picture and microscopic image of the sample printed using the gray scale image method are shown in Fig. 15 (c) and (d). The profile of the line region same as the region in Fig. 15 (b) which was contacted with the microgroove of the constrained surface, is plotted as the red curve in Fig. 16. It can be seen from Fig. 15 (d) and (e) that with the gray scale image method, the imprinted texture feature could be eliminated. It indicates that effects of the microgroove in the PDMS constrained surface on the surface finish of the printed part could be eliminated by the gray scale image method. Additionally, the surface roughness of 75 mm diameter cylinder, mechanical gear and square samples fabricated with textured PDMS surface were measured, as listed in Table 1. It can be seen that the gray scale image method is a feasible approach to eliminating the imprinted texture and improving the surface roughness of printed parts.

Table 1. Roughness measurements of parts fabricated with textured constrained surface

Models	Ra (um)	Rq(um)	Rz(um)
Square sample (before eliminating textures)	0.58167	0.39486	23.754
Square sample (after eliminating textures)	0.25126	0.33688	2.224
75 mm diameter cylinder	0.792	0.98444	24.055
Mechanical gear	0.27684	0.35599	25.155

5. Conclusions

A novel constrained surface texturing method for separation force reduction in projection stereolithography systems is developed in this study. Analytical models indicate that by modifying the constrained surface with radial microgroove patterns, the separation force during printing process could be reduced greatly. Several PDMS samples with microgroove patterns are prepared using micro milling and femtosecond laser micromachining technologies. Separation forces during the printing process using textured constrained surfaces are measured and compared with the forces during printing process using the conventional non-textured constrained surface. Multiple parts have been built successfully with the developed Projection SL process based on textured PDMS constrained surfaces. Experimental results verified the effectiveness of constrained surface texturing approach in reducing separation forces and fabricating 3D objects. Furthermore, this study demonstrated advantages of the proposed textured constrained surface in Projection SL on fabricating parts with large solid cross section areas, which are very challenging or even impossible with current constrained surface Projection SL technology due to over-large separation forces.

Future work will be conducted to further optimize surface texture design, and develop the gray scale image method for eliminating the texture imprinting problem for printing complicated geometries with high surface finish.

Acknowledgement

This material is based upon work supported by the National Science Foundation under Grant No. 1563477. The authors would like to also acknowledge the Nanotechnology Core Facility of the University Of Illinois at Chicago campus for training on and usage of the Bruker-Nano Model Contour GT-K Optical Profilometer.

References

[1] K. Ikuta et al. "Real three dimensional micro fabrication using stereo lithography and metal molding." MEMS: 1993, 42-47

[2] H, He et. al. Effect of Surface Texturing on Separation Force in Projection Stereolithography, 11th International Conference on Micro Manufacturing, ICOMM 2016, Irvine, California, March 29-31, 2016

[3] Denken Corp., SLP-4000 Solid Laser Diode Plotter, Product Brochure, Denken Corporation, Japan, 1997.

[4] Y. Pan et. al, "A Fast Mask Projection Stereolithography Process for Fabricating Digital

Models in Minutes.” J. Mfg. Sci. Eng., Vol. 134, No. 5, pp. 051011, 2012
[5] P.M. Lambert et al., "Design Considerations for Mask Projection Microstereolithography Systems." SFFS: 2013, 111-130.
[6] J. Hendrik et al., "Apparatus and method for the non-destructive separation of hardened material layers from a flat construction plane." U.S. Patent 7,438,846, issued October 21, 2008.
[7] D. J. Kukulka et al. "Effect of rigidized textured surfaces on heat transfer and fouling of enhanced tubes," Chem. Eng. Trans., 2009; 18: 575-580.
[8] S. Srinivasan et al."Sustainable Drag Reduction in Turbulent Taylor-Couette Flows by Depositing Sprayable Superhydrophobic Surfaces," Phys. Rev. Lett., 2015; 114: 014501.
[9] L. Xu, "Liquid drop splashing on smooth, rough, and textured surfaces," Phys. Rev. E, 2007; 75(5): 056316.
[10] D. Quere et al. "Slippy and sticky microtextured solids," Nanotechnology, 2003; 14(10: 1109-1112.
[11] E. M. Nicolaiewsky et al. "Liquid flow over textured surfaces. 1. Contact angles," Ind. Eng. Chem. Res. 1999; 38(1): 284-291.
[12] H. Bruus, Theoretical Microfluidics. Oxford: Oxford University Press: 2008, 74-78.
[13] Tumbleston, John R., David Shirvanyants, Nikita Ermoshkin, Rima Janusziewicz, Ashley R. Johnson, David Kelly, Kai Chen et al. "Continuous liquid interface production of 3D objects." Science 347, no. 6228 (2015): 1349-1352.
[14] Q. Bian et al. “Femtosecond laser ablation of indium tin-oxide narrow grooves for thin film solar cells.” Opt. & Laser Tech., 2013; 45: 395–401.
[15] Y. Pan, et al. "Study of separation force in constrained surface projection stereolithography." Rapid Prototyping Journal 23.2 (2017): 353-361.